On the Determination of the Diffusivity of CO2 in Aqueous and NonAqueous Solvents

Hogendoorn, J.A.; Vas Bhat, R.D.; Versteeg, G.F.

Published in:
Chemical Engineering Communications

DOI:
10.1080/00986440213884

Publication date:
2002

Chem. Eng. Comm., 189: 1009–1037, 2002

0098-6445/02 $12.00 + .00
DOI: 10.1080/00986440290012492

ON THE DETERMINATION OF THE DIFFUSIVITY OF CO_2 IN AQUEOUS AND NONAQUEOUS SOLVENTS: INVESTIGATIONS WITH LAMINAR JETS AND WETTED WALL COLUMNS

J. A. HOGENDOORN
R. D. VAS BHAT
G. F. VERSTEEG

Department of Chemical Engineering, University of Twente, Enschede, The Netherlands

The diffusivity of CO_2 in ethanol, n-heptane and methyl tertiary butyl ether (MTBE) has been determined using a laminar jet reactor and a wetted wall column at two temperatures (293 K and 298 K). The reactors have been operated in the laminar and transition regime. In the transition regime, the effective diffusivity of CO_2 was found to increase with Reynolds number, which could be explained by the increasing contribution of eddy diffusivity to the overall mass transfer. However, even in the laminar regime, the molecular diffusivity of CO_2 was found to vary with experimental conditions, i.e., the Reynolds number. It has been observed that the value of D_{CO_2} reduces with increasing Re in the case of ethanol, while the opposite trend is observed for n-heptane. These effects can be (partially) explained by accounting for combined molecular and eddy diffusivity within the laminar regime as proposed by the mass transfer model of King (1966). To the knowledge of the authors, these effects of gas absorption in nonaqueous/organic solvents have not been reported earlier. The present findings indicate that data on gas absorption in these types of systems should be used with caution.

Keywords: Diffusivity; Laminar jet; Wetted wall; Carbon dioxide point

Received 12 September 2000; in final form 23 April 2001.

Address correspondence to G. F. Versteeg, Department of Chemical Engineering, University of Twente, P.O. Box 217, 7500 AE Enschede, The Netherlands. Tel.: 0031-534893027, Fax: 0031-534894774. E-mail: g.f.versteeg@ct.utwente.nl

INTRODUCTION

Gas-liquid mass transfer forms an integral part of a number of industrial processes. The various theoretical models that describe gas-liquid mass transfer usually differ only in the dependence of the mass transfer coefficient on diffusivity of the gaseous species. In general, the variation of the liquid phase mass transfer coefficient k_L with diffusivity D_A can be denoted as

$$k_L = \xi D_A^{\psi} \tag{1}$$

where ξ is a function of the hydrodynamic parameters of the reactor under consideration while the value of the exponent ψ depends on the mass transfer theory applicable. Ψ may be a constant, as in case of the film theory (Whitman, 1923) ($\psi = 1$). The Higbie penetration theory (Higbie, 1935) and Danckwerts's surface renewal theory (Danckwerts, 1951) both predict an exponent of 0.5. Some models also predict a variable exponent, depending on the intensity of turbulence in the vicinity of the gas-liquid interface. The film-penetration model postulated by Toor and Marchello (1958) predicts a value of ψ in the range of 0.5–1.

Thus, it is clear that, depending on the theory applied to describe the mass transfer process, the accurate determination of the value of diffusivity is essential. Errors in determination of the diffusion coefficient are amplified when dealing with diffusion-controlled processes such as instantaneous gas-liquid reactions. Although correlations for estimating the diffusion coefficient have been reported in literature (among others Reid et al. (1988)), these do not substitute (where possible) the experimental determination of this parameter for the system under consideration. A standard approach to determine this value is by measuring the absorption rate R_A of the gas in the liquid under consideration.

$$R_A = k_L a V_L (\textit{driving force}) \tag{2}$$

where a is the gas-liquid interfacial area and V_L is the total liquid volume or the volume of the reaction phase, depending on the manner in which a is defined.

This method requires the physical absorption of the gas into the liquid phase and cannot be directly measured in case of a reaction between the gas and liquid species. From Equation (2) the value of D_A can be calculated via k_L (using Equation 1) if the exact hydrodynamic characteristics (ξ) of the reactor are known. These include the film thickness (film theory), the gas-liquid contact time (Higbie penetration theory (Higbie, 1935)) or the surface renewal parameter (Danckwerts's surface renewal theory (Danckwerts, 1951)). Typical laboratory reactors

with well-defined and adjustable hydrodynamic characteristics that are used for the determination of diffusivity include the stirred cell, laminar jet reactor and the wetted wall column. The aim of the present study is to:

- Provide information on the diffusivity of CO_2 in non-aqueous solvents for ambient conditions.
- Critically analyze the data obtained by the use of model contactors and their usefulness for the determination of the diffusion coefficient.

The present study includes two of these model gas-liquid contactors, namely, the laminar jet and the wetted wall column.

LAMINAR JET REACTOR

Laminar liquid jets have been often used in the determination of diffusion coefficients in gas-liquid systems in the case of sparingly soluble gases. Since these jets can be approximated as cylindrical rods of liquid moving at a fixed velocity, they provide accurate hydrodynamics for gas absorption since the gas-liquid contact time can be easily determined. A laminar jet reactor consists of a capillary tube through which the liquid under investigation is ejected into an atmosphere of gas. The liquid is collected in a receiver where it flows out of the reactor. Gas is absorbed into the liquid during the contact time, which is monitored in order to determine the gas absorption rate. Since the gas-liquid interfacial area is well defined and known (assuming the jet to behave as a cylindrical rod of liquid), the gas flux can also be determined. An attractive feature of the laminar jet is the wide range of contact times that can be achieved (10^{-3} to $7\ 10^{-2}$ s). This provides a wide flexibility while studying gas-liquid physical absorption, but also simultaneous absorption with chemical reaction in the liquid phase.

The need for the liquid jet to be laminar in flow before leaving the nozzle is to provide a uniform radial velocity profile after ejection from the nozzle. In this manner, diffusion of the gas into the liquid jet is not influenced by internal velocity gradients. On leaving the nozzle, the parabolic velocity profile characteristic of laminar flow relaxes under the influence of body forces, while the drag force of the surrounding medium (the gas phase) on the liquid can be neglected. Traditionally, the transition from laminar to turbulent flow in a long tube has been characterized by the critical Reynolds number Re_C, defined as

$$\mathrm{Re}_C = \frac{\rho_L U d_T}{\eta_L} \tag{3a}$$

where d_T is the tube diameter and U is the average liquid velocity in the tube.

The lower boundary for transition from laminar to turbulent flow in pipes is around 2300 (Schlichting, 1968). However, the liquid flow is modified while being ejected through the nozzle so that, in practice, the critical Reynolds number has been found to depend on nozzle diameter and geometry as well. As reported by van de Sande and Smith (1976), for nozzle diameters of 2.5 mm and 5 mm and with conical tapered edges the following expression holds (water into air system):

$$\mathrm{Re}_C = 12000\left(\frac{L_n}{d_n}\right)^{-0.3} \tag{3b}$$

where L_n is the nozzle length and d_n is the nozzle diameter.

A fundamental description of the hydrodynamics of laminar liquid jets has been reported previously by, among others, Scriven and Pigford (1959) and Duda and Vrentas (1967).

Gas Absorption in Laminar Liquid Jets

The laminar jet reactor has been a commonly used laboratory tool for measuring the absorption of sparingly soluble gases. The short contact time characteristics of laminar jet reactors justify the use of the penetration theory to describe gas-liquid mass transfer. If the penetration depth of the gas into the jet is very small in comparison with the jet radius, then the curvature of the laminar jet can be neglected and the absorption may be described as that into an infinite stagnant slab. For this assumption to hold, the following criterion should be met.

$$\frac{D_A\tau}{R^2} <\approx 0.1 \tag{4}$$

where τ is the gas-liquid contact time, R is the jet radius and A is a sparingly soluble gas under investigation.

The unsteady state gas absorption of A into the liquid jet may be described by

$$\frac{\partial C_A}{\partial t} = D_A\frac{\partial^2 C_A}{\partial x^2} \tag{5a}$$

where C_A is the liquid phase concentration of component A.

Equation (5a) is solved with the following initial condition

$$t = 0; \quad x \geq 0 \Rightarrow C_A = C_{A,0} \tag{5b}$$

and boundary conditions

$$t > 0; \quad x = 0 \Rightarrow C_A = C_{A,i} \tag{5c}$$

$$t > 0; \quad x \to \infty \Rightarrow C_A = C_{A,0} \tag{5d}$$

where $C_{A,0}$ is the initial concentration of A in the liquid and $C_{A,i}$ is its interfacial value, assumed to be at equilibrium with the gaseous phase.

Solving Equation (5a) under conditions (5b–5d) for the time averaged flux N_A across the gas-liquid interface results in (Higbie, 1935)

$$N_A = 2\sqrt{\frac{D_A}{\pi\tau}}(C_{A,i} - C_{A,0}) \tag{6a}$$

The gas-liquid contact time τ is assumed to be equal to the liquid residence time determined by

$$\tau = \frac{V_J}{\phi_L} = \frac{L_J\left(\frac{\pi}{4}d_J^2\right)}{\phi_L} \tag{6b}$$

where the subscript J refers to the liquid jet and ϕ_L is the liquid flow rate.

Combining equations (6a) and (6b) provides the absorption rate R_A of a gas in a liquid jet as

$$R_A = 4(C_{A,i} - C_{A,0})\sqrt{D_A\phi_L L_J} \tag{6c}$$

Equation (6c) is used to experimentally determine the diffusion coefficient of A in a liquid.

Description of Setup

The setup used to study gas absorption in a laminar jet reactor is given in Figure 1. Demineralized water (or other liquids under investigation) was taken in a 40 liter polymer storage tank and degassed overnight by bubbling through with nitrogen. Degassed liquid was then pumped via a centrifugal pump with a pulsation free head into a thermostat bath where it was heated to a predetermined temperature. The liquid was then led to

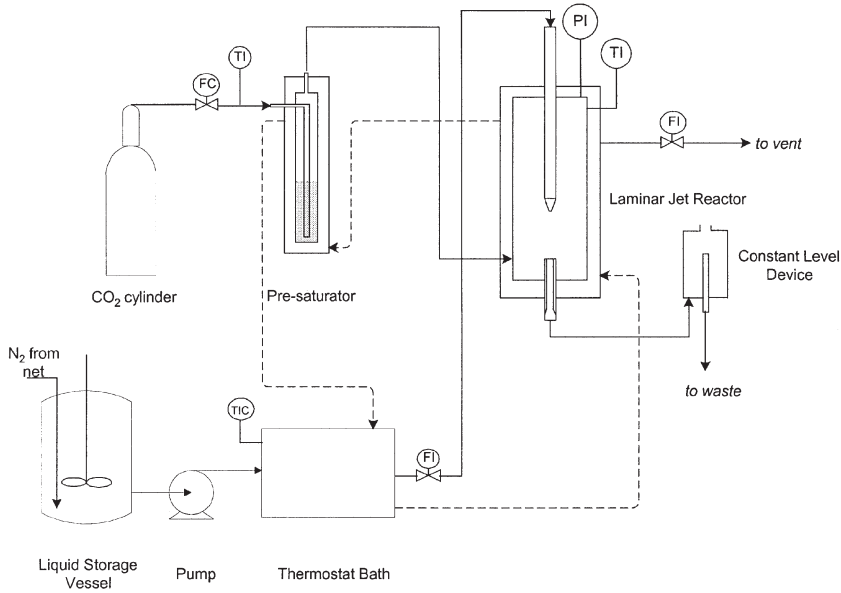

Figure 1. Experimental setup used for studying gas absorption in a laminar jet reactor.

the inlet of the laminar jet reactor via a liquid flow meter. Varying the pump flow rate by means of an external frequency controller controlled the liquid flow rate.

The laminar jet reactor consisted of a double-walled glass vessel with the liquid inlet consisting of a 30 cm long glass tube that ended in a tapered nozzle with a diameter of 1 mm and a length of 8 mm. The liquid ejected from the nozzle was caught by a receiver having a diameter of 1.2 mm from where it left the reactor. The inlet liquid tube was attached to a fixed support while the lower receiver was attached to a movable table that could be adjusted with a precision of 0.05 mm in a plane perpendicular to the inlet nozzle. The receiver was thus adjusted until the jet entered the receiver. The jet length could be adjusted between 4 and 8 cm by moving the liquid inlet tube vertically. Jet height and diameter were measured by means of a cathetometer (least count = 50 μm). The double wall of the reactor facilitated in heating the reactor contents and maintaining the same temperature as the water inlet. Some characteristics of the nozzle and receiver are shown in Figure 2.

Liquid exiting the reactor was discharged into a constant level device. This was a glass bulb open to atmospheric pressure on one end and containing a central overflow tube. The device could be moved vertically along a scale so that the exit of the jet could be adjusted to prevent gas entrainment into the receiver or spillage of the liquid out of the receiver.

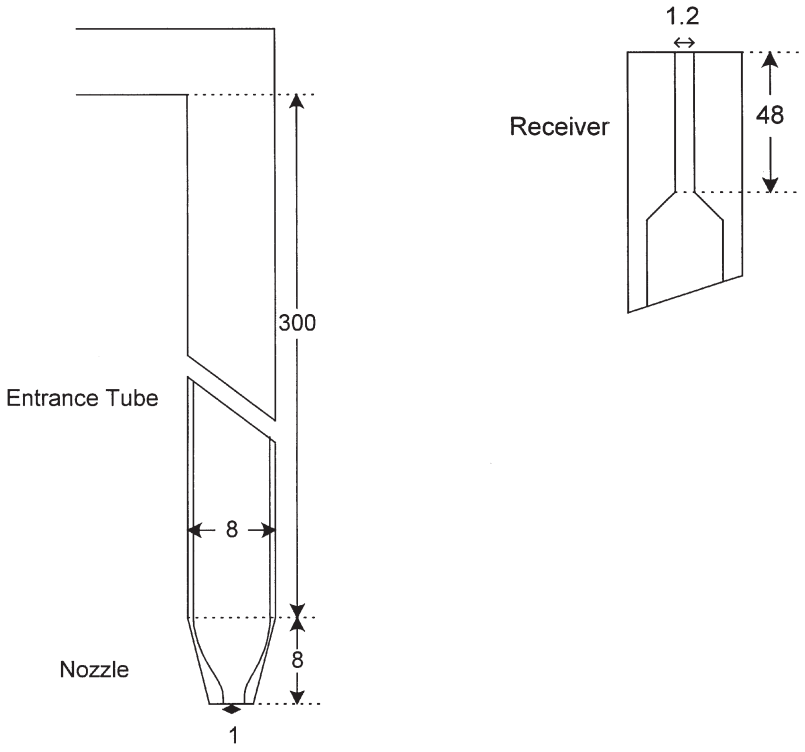

Figure 2. Details of nozzle and receiver in the laminar jet reactor.

Liquid leaving the overflow tube was collected for disposal. Temperature of the liquid was measured at the reactor inlet and outlet.

CO_2 from a gas cylinder was bubbled through demineralized water (or the liquid under investigation) to pre-saturate the gas before passing it through a thermal mass flow meter, after which it was led through the reactor. Temperature of the liquid in the presaturator was maintained identical to the temperature of the liquid at the reactor inlet. Further, the gas tubing was lined with an electric heating element to maintain a constant gas temperature throughout the apparatus. The gas temperature was measured at the reactor inlet. The outlet gas flow rate was controlled at the reactor inlet while it was measured at the reactor outlet only.

Experimental Procedure. The liquid to be investigated was degassed overnight by bubbling nitrogen through the storage vessel. Before starting an absorption experiment, the setup was purged by passing CO_2 for 15 min so as to eliminate all inerts from the gas phase. The liquid was allowed to flow into the reactor and its flow rate was controlled by varying the pump speed. Liquid temperature was fixed using the

thermostat bath. Once steady state with respect to the liquid was achieved, the constant level device was adjusted to obtain a steady jet with no gas entrainment at the exit. Jet dimensions were then measured using the cathetometer.

The temperature of the gas tubing was also set so that the temperature of the gas and liquid entering the reactor was identical. Gas flow rate was fixed at a predetermined set-point and the entire setup was allowed to reach steady state. The liquid flow rate was noted, along with reactor temperature and pressure. For the gas, the reactor outlet temperature and flow rate was measured. The liquid flow was then stopped and the gas flow at the exit of the reactor was measured until it rose to a steady state. Difference in gas flow rate with and without the flow of liquid was used to determine the gas absorbed into the liquid.

Data Analysis. Before using the laminar jet apparatus to determine diffusivity of gases in liquids, it was necessary to determine if the constraint provided by Equation (4) was met. It was found that for all gas-liquid systems presented in this study, this was true. Further, the value of Re_C was found to be below 3000, which is well below the value predicted by Equation (3b) for the geometry of the nozzle used in this study. Equation (6c) was used in the determination of the diffusion coefficient of CO_2 in liquids. In order to determine the interfacial concentration, the gas phase mass transfer resistance was assumed to be negligible. This assumption seems justified since the apparatus was sufficiently purged with CO_2 to ensure the removal of all inerts. Additionally, even though the CO_2 was presaturated with the liquid, the corresponding partial pressure of the liquid component was low under the operating conditions.

The interfacial concentration of CO_2 in water was determined using the correlation provided by Versteeg and van Swaaij (1988a) that is valid in the range of 0−1 bar.

$$\mathrm{He}_{\mathrm{CO_2,H_2O}} = 3.59 \cdot 10^{-7} exp\left(\frac{2044}{T}\right)$$
$$\text{with } \mathrm{C}_{\mathrm{CO_2},i} = \mathrm{He}_{\mathrm{CO_2,H_2O}} \cdot p_{G,\mathrm{CO_2,i}} \tag{7}$$

where He is defined in $\mathrm{mol\,m^{-3}\,Pa^{-1}}$. The exact partial pressure of CO_2 in the gas phase of the reactor was taken from the total reactor pressure corrected for the vapor pressure of water at that temperature. Knowing the partial pressure of CO_2, it was possible to determine $C_{A,i}$ required in Equation (6c). All other physical parameters were taken from Daubert and Danner (1985). In the case of diffusivity of CO_2 in water, the diffusivity determined here was compared with the experimentally determined correlation provided by Versteeg and van Swaaij (1988a) measured at 1 bar

$$D_{CO_2,H_2O} = 2.35 \cdot 10^{-6} exp\left(\frac{-2119}{T}\right) \quad (8)$$

Results

CO_2 - Water. The variation in diffusivity of CO_2 in water with temperature of the liquid is shown in Figure 3. The diffusion coefficient determined using the procedure described before is comparable to that given in Equation (8). This latter correlation was obtained by fitting diffusivity data on the CO_2-water system that was previously published in open literature. It is clear that the data reported in the present study is well within the experimental accuracy associated with the measurement.

Since the jet used in the present study has been found to be laminar at the nozzle exit, the liquid velocity profile is flat for most of the jet length. Consequently, it could be assumed that the diffusion coefficient measured here is equal to the molecular diffusion coefficient while neglecting the contribution of eddy diffusion. This is confirmed by the small deviation between the diffusion coefficient determined here and the empirical correlation reported by Versteeg and van Swaaij (1988a). Another method of confirming this is to study the influence of the jet Reynolds number

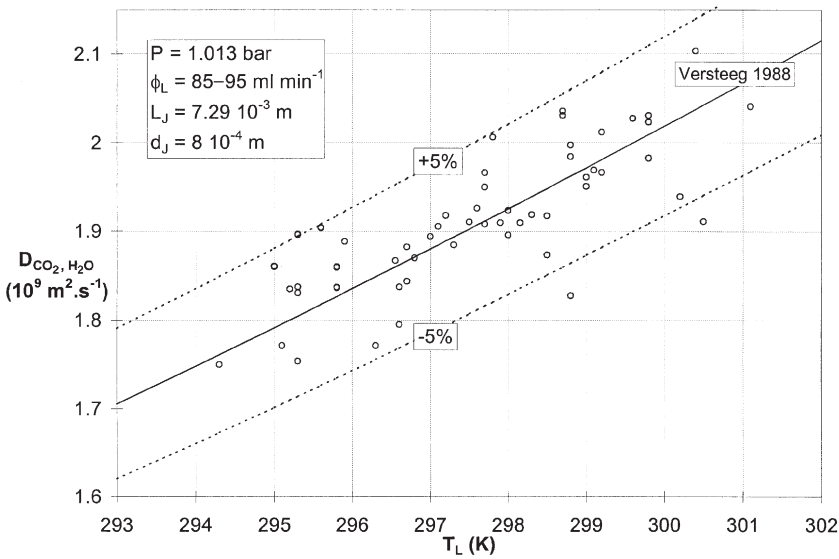

Figure 3. Diffusion coefficient of CO_2 in water as a function of temperature (laminar jet reactor). Full line represents correlation presented by Versteeg and van Swaaij (1988a).

(Re_J) on the diffusivity. The contribution of the eddy diffusion coefficient (if any) on the overall diffusivity is expected to increase at higher values of Re_J. Assuming a uniform liquid velocity along the length of the jet, the jet Reynolds number may be defined as:

$$Re_J = \frac{d_J U_J \rho}{\eta} \tag{9}$$

Liquid density and viscosity have been determined at the inlet liquid temperature.

The diffusivity of CO_2 in water at varying values of Re_J is plotted in Figures 4a and 4b. At lower values of Re_J (typically < 2500; Figure 4a), a steady, slight increase in diffusivity with Re_J is observed. This trend is not reproduced for $Re_J > 2500$ (Figure 4b) where the diffusivity is, within experimental accuracy, constant over the range of Reynolds numbers studied. Thus, the results presented here seem to suggest that, for the process conditions under investigation, there is a transition in the absorption behavior of CO_2 in water at a jet Reynolds number of around 2500. This effect cannot be explained because:

- All experiments are carried out well within the critical Reynolds number as defined by Equation (3b). The value of Re_C determines the region where the liquid ejected through the nozzle is turbulent.

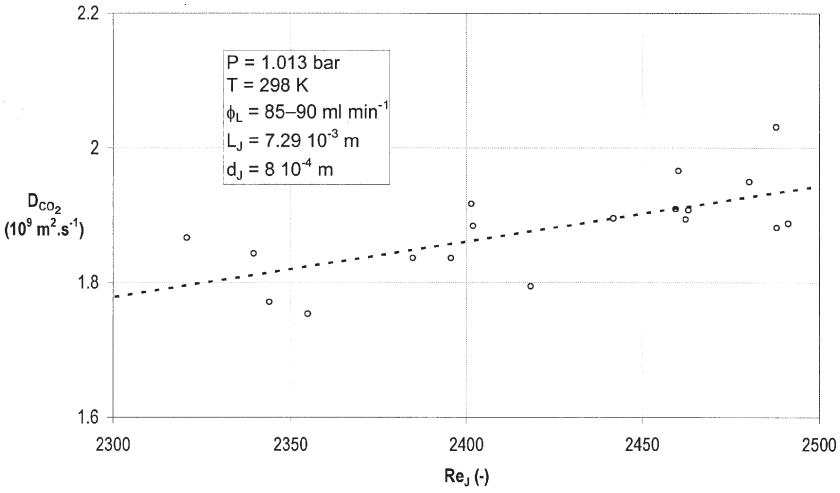

Figure 4a. Influence of the jet Reynolds number on diffusivity (laminar jet reactor). CO_2-water system; low Reynolds numbers.

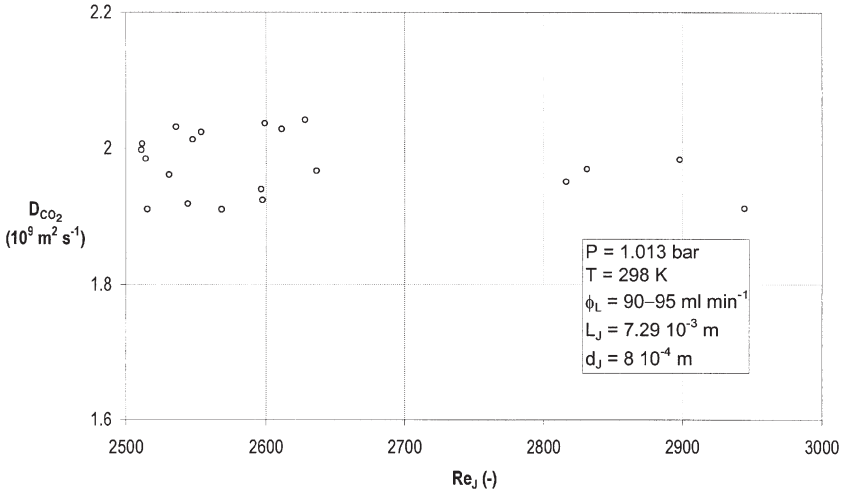

Figure 4b. Influence of the jet Reynolds number on diffusivity (laminar jet reactor). CO_2-water system; high Reynolds numbers.

- At lower values of Re_J, the system could be assumed to be completely laminar. In this regime a flat profile of D_{CO_2} would be expected since there cannot be an effect of the contactor hydrodynamics on the molecular diffusion coefficient. Thus, it is not possible to explain the monotonic increase in the value of D_{CO_2} as observed in Figure 4a.
- The increase in turbulence at higher values of Re_J would result in a monotonic increase in diffusivity due to the enhancement provided by eddies to molecular diffusivity. However, it would not explain the flattening of the profile at higher values of Re_J as observed in Figure 4b.

CO_2-Ethanol. As for the previous system, the influence of Re_J on the diffusivity of CO_2 in an organic solvent was studied. Solvent grade ethanol (96%) was chosen for this purpose. The solubility of CO_2 in ethanol has been reported by Fogg and Gerrard (1991). The molar solubility of CO_2 ethanol at a partial pressure of 1 atm. is given by:

$$ln(x_{CO_2}) = -22.278 + \left(\frac{2027.1}{T}\right) + 1.8532\ln(T) \tag{10}$$

where x_{CO_2} is the mole fraction of CO_2 in ethanol at a temperature T. Using the same experimental procedure as described above, the diffusion coefficient of CO_2 was determined using Equation (6c) at a fixed temperature of 298 K. Experiments were carried out at different gas-liquid contact times (τ) by varying the liquid flow rate and the jet length (L_J) in

the range of $900 \leq Re_J \leq 1100$. From a total of 40 experiments, an average value of $2.91\,10^{-9}\,m^2\,s^{-1}$ ($\sigma^2 = 0.25$) was obtained for the diffusion coefficient. This value was higher when compared to the diffusion coefficient predicted by the Wilke-Chang correlation using an association factor of 1.5 for the CO_2-ethanol system (Reid et al., 1988). A value of $1.94\,10^{-9}\,m^2\,s^{-1}$ was calculated with this correlation. Table I gives an overview of other values reported in literature for the diffusivity of CO_2 in ethanol at 298 K.

In order to check the reason for the higher value of diffusion coefficient obtained experimentally, the diffusivity was plotted as a function of the jet Reynolds number (Figure 5). As seen from the figure, there is a sharp reduction in diffusivity with an increase in Re_J. This trend is contrary to that observed in the case of water (see Figure 4a). Once again, an average value for experiments carried out with $Re_J < 950$ yields an average diffusion coefficient of $3.25\,10^{-9}\,m^2\,s^{-1}$ while $Re_J > 1050$ results in an average value of $2.71\,10^{-9}\,m^2\,s^{-1}$. On comparing with reported values of D_{CO_2} in ethanol (see Table I), it would seem that a "true" diffusivity can be measured in the lower range of Re_J for a laminar jet reactor.

From the results obtained above with the laminar jet reactor it can be concluded that the use of this model contactor does not result in a uniquely measured diffusion coefficient. The results are strongly dependent on the experimental conditions. This effect was not expected and cannot be explained from fundamental flow phenomena. In order to investigate these observations further, the absorption of CO_2 into demineralized water and organic solvents was carried out in a laboratory-scale wetted

Table I Comparison of reported diffusion coefficients of CO_2 in ethanol at 298 K

Method	D_{CO_2} ($10^9\,m^2\,s^{-1}$)	Reference
Laminar jet	3.66	Tang and Himmelblau (1965)
Diaphragm cell	4.04	Takeuchi et al. (1975)
Wetted wall column	4.50	Simons and Ponter (1975)
Wetted wall column	3.31	Alvarez-Fuster et al. (1981)
Diaphragm cell	3.86	Takahashi et al. (1982)
Wetted wall column	2.69‡	Versteeg and van Swaaij (1988b)
Taylor dispersion	4.11	Snijders et al. (1995)
Wetted wall column	2.49	present study
Laminar jet	2.91†	present study
Wilke-Chang	1.94	present study

† $Re_J < 950$; $D_{CO_2} = 3.25\,10^{-9}\,m^2\,s^{-1}$.

† $Re_J > 1050$; $D_{CO_2} = 2.71\,10^{-9}\,m^2\,s^{-1}$.

‡ Diffusivity calculated with value of m_{CO_2} experimentally determined in this study.

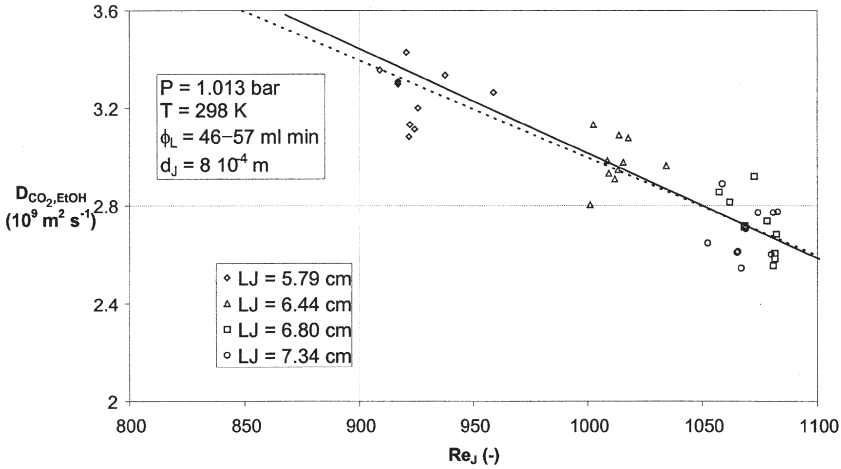

Figure 5. Influence of the jet Reynolds number on diffusivity. CO_2-ethanol system: laminar jet reactor. Average $D_{CO_2} = 2.91\,10^{-9}\,m^2\,s^{-1}$.

wall column. Such reactors have also been used previously to characterize mass transfer in industrial reactors such as a falling film reactor. The experimental analysis and results for the various gas-liquid systems investigated are presented below.

WETTED WALL COLUMN

Wetted wall columns possess the advantage that the interfacial area can be easily determined from reactor geometry; hence, these contactors find extensive usage as laboratory model contactors for the investigation of mass transfer in gas-liquid systems. A comprehensive review of gas-liquid systems investigated using this contactor has been provided by Spedding and Jones (1988). Mass transfer characteristics of wetted wall columns are expressed in the form of a Sherwood correlation of the type (Spedding and Jones, 1988; Nielsen et al., 1998):

$$Sh = c_1 \mathrm{Re}^{c_2} Sc^{c_3} \tag{11a}$$

where the dimensionless numbers are defined as:

$$Sh = \frac{k_L d_P}{D_A}; \quad \mathrm{Re}_P = \frac{\Gamma \rho_L}{\eta_L} \quad \text{and} \quad Sc = \frac{\eta_L}{\rho_L D_A} \tag{11b}$$

d_P represents the pipe diameter and Γ is the volumetric liquid load, defined as the liquid flow rate per unit wetted perimeter of the column.

Such correlations have been reported previously (Nielsen et al., 1998) for high Reynolds numbers. However, an important drawback is that they can be used only for a falling film with a length equal to that for which they were experimentally determined. Thus, in order to use correlations such as that given in Equation (11a), it is necessary to compensate for the effect of film length on the mass transfer.

Gas Absorption in Wetted Wall Columns

For the case of falling films with a nonrippling surface, it can be shown that for laminar flow (parabolic velocity profile), the Sherwood correlation is dependent on the diffusivity of the gas phase component into the liquid film. This is denoted by Equation (12) (Spedding and Jones, 1988; Nielsen et al., 1998; Treybal, 1980).

$$Sh = \sqrt{\frac{2}{\pi}} \cdot 3^{2/3} \cdot \left(\frac{\eta_L^2}{\rho_L^2 g}\right)^{1/6} \cdot \mathrm{Re}_P^{2/3} \cdot Sc^{1/2} \cdot L^{-1/2} \tag{12}$$

where L is the length of the falling film of the wetted wall column.

Such a correlation could be used to characterize mass transfer in wetted wall columns with liquid flowing in the laminar regime. However, it is extremely difficult to restrict the formation of ripples on the liquid surface. Such waves contribute to an enhancement in mass transfer by a possible influence on the molecular diffusivity by turbulence. However, for a falling film, the transition to turbulent flow occurs at Reynolds numbers of about 400–800 while the large increase in mass transfer has already been observed for Reynolds numbers as low as about 30 (Yoshimura et al., 1996).

Thus, the flow of liquid in a wetted wall column can be classified into an operating zone where the flow is nonrippling and laminar followed by a nonideal zone characterized by surface waves and turbulence. For the experimental setup used in the present study, the length of the operating zone is dependent on the liquid flow rate and can be correlated with a linear relation of the type:

$$L_{op} = c_4 + c_5 \mathrm{Re}_P \tag{13}$$

Since the flow in the operating zone is completely laminar, the diffusion coefficient measured based on the absorption into this zone is the molecular diffusion coefficient of the gas and is independent of the liquid flow rate.

For short gas-liquid contact times (i.e., fulfilling Equation 4) it can be easily shown that the average gas absorption flux N_A is denoted by (see also Equation 6 and (Higbie, 1935)):

$$N_A = 2C_{A,i}\sqrt{\frac{D_A v_i}{\pi L}} \tag{14}$$

where v_i is the velocity of the liquid film at the interface.

The gas absorption rate can be determined by assuming the falling film to be a perfect cylinder with an effective diameter of $(d_p + 2\delta)$, where δ is the thickness of the falling film. By multiplying the flux given by Equation (14) with the available surface area the following equation is obtained.

$$R_A^2 = 4\pi(d_P + 2\delta)^2 C_{A,i}^2 D_A v_i L \tag{15a}$$

or, in terms of the volumetric absorption rate W_A,

$$W_A^2 = 4\pi(d_P + 2\delta)^2 m_A^2 D_A v_i L \tag{15b}$$

where m_A is the gas partition coefficient defined as

$$m_A = \frac{C_{A,i}}{C_{A,G}} \tag{15c}$$

The value of m_A needs to be experimentally determined for the temperature at which the gas-liquid system is being investigated. Equation (15b) can be used to determine the molecular diffusion coefficient by plotting the square of the volumetric gas absorption rate against the film length. For flow of the liquid in the laminar regime with no slip at the wall, the liquid flows with a parabolic velocity pattern with maximum velocity at the interface. Under these conditions and assuming that the flow is along a flat plate, it can be shown that the value of v_i is given by (Treybal, 1980),

$$v_i = \frac{1}{2} \cdot 3^{2/3} \cdot \left(\frac{\rho_L g}{\eta_L}\right)^{1/3} \cdot \Gamma^{2/3} \tag{16a}$$

while the thickness of the falling film by:

$$\delta = \left(\frac{3\eta_L}{\rho_L g}\right)^{1/3} \Gamma^{1/3} \tag{16b}$$

Within the nonideal zone of the falling film, the liquid surface is no longer ripple-free and the diffusion coefficient measured is an effective diffusion coefficient that consists of the contributions of the molecular diffusion coefficient D_A and an addition, ΔD, which could arise due to a number of reasons, namely:

- An increase in the gas-liquid interfacial area by the formation of ripples
- An additional transport mechanism within the liquid phase due to turbulence
- A change in the parabolic velocity profile of the liquid

It should be noted, however, that the transition to the nonideal zone usually cannot be observed visually. Thus the effective diffusion coefficient is defined as

$$D_{A,eff} = D_A + \Delta D \tag{17}$$

However, the relationship between W^2 and the film length L can still be used to determine the effective diffusion coefficient from the slope of Equation (15b). The length of the operating zone can be determined from the intercept of the y-axis.

Finally, at the exit of the liquid film lies a stagnant film layer where no replacement of the liquid occurs with time. Once this layer is saturated with the gas, it no longer contributes to absorption. The theoretical pattern that can be expected for gas absorption along the length of a falling film is given in Figure 6. The lengths of the various zones can be determined by extrapolating the absorption profiles to the axis.

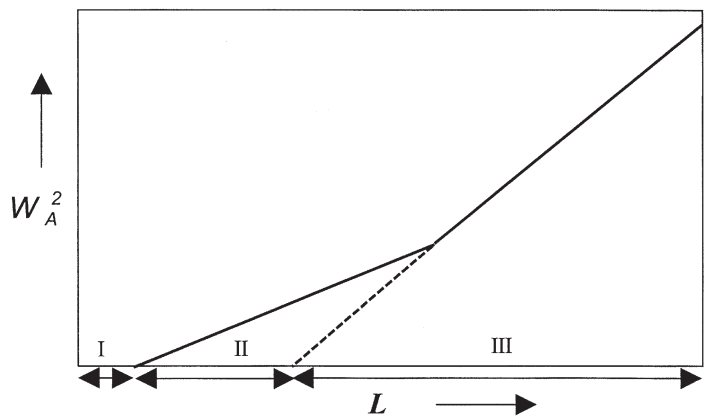

Figure 6. Typical absorption pattern in a wetted wall column. Plotted is the square of the volumetric gas absorption rate against the length of the film. I, Stagnant zone; II, Operating zone; III, Nonideal zone.

Description of Setup

The experimental setup for absorption in a wetted wall column is shown in Figure 7, while details of the model contactor itself are given in Figure 8. The wetted wall column consists of a hollow round metal tube with a diameter of 17.6 mm. The liquid flows down its outer surface as a falling film. The liquid itself enters the reactor at the bottom of the tube and flows along the tube interior to the top, where it is directed to the outer tube perimeter by means of a liquid distributor, which consists of a second tube placed above the first. The bottom part of this tube is drilled so that the inlet tube can be placed within the liquid tube to leave an annular opening between the two tubes, as shown in Figure 8. The tubes are placed in a double-walled glass vessel with a gas inlet and outlet for liquid. The temperature of the contactor is regulated by passing water from a thermostat bath. In addition, it is also completely isolated from the atmosphere except via the fluid inlet and outlet tubes.

The liquid under investigation was fed from a storage vessel to an overhead tank by means of a peristaltic pump. The overhead tank was maintained at a constant liquid level by means of an overflow tube. Liquid from this tank was passed through a thermostat bath to bring it to the desired temperature, and then fed to the reactor inlet. The liquid inlet was fitted with a flowmeter so that the liquid flow could be accurately measured. The overhead tank provided a constant liquid pressure and helped to dampen any fluctuations in the liquid flow. The liquid passed through the inside of the inlet tube after which it formed a film along the

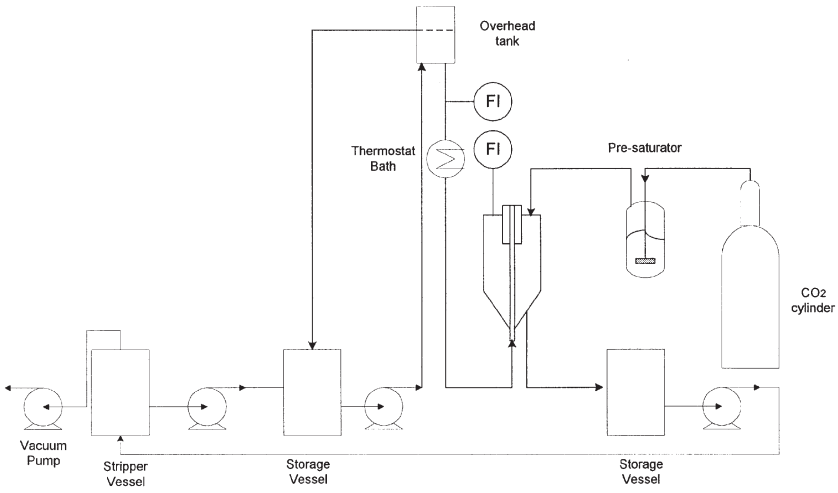

Figure 7. Experimental setup for studying gas absorption in a wetted wall column.

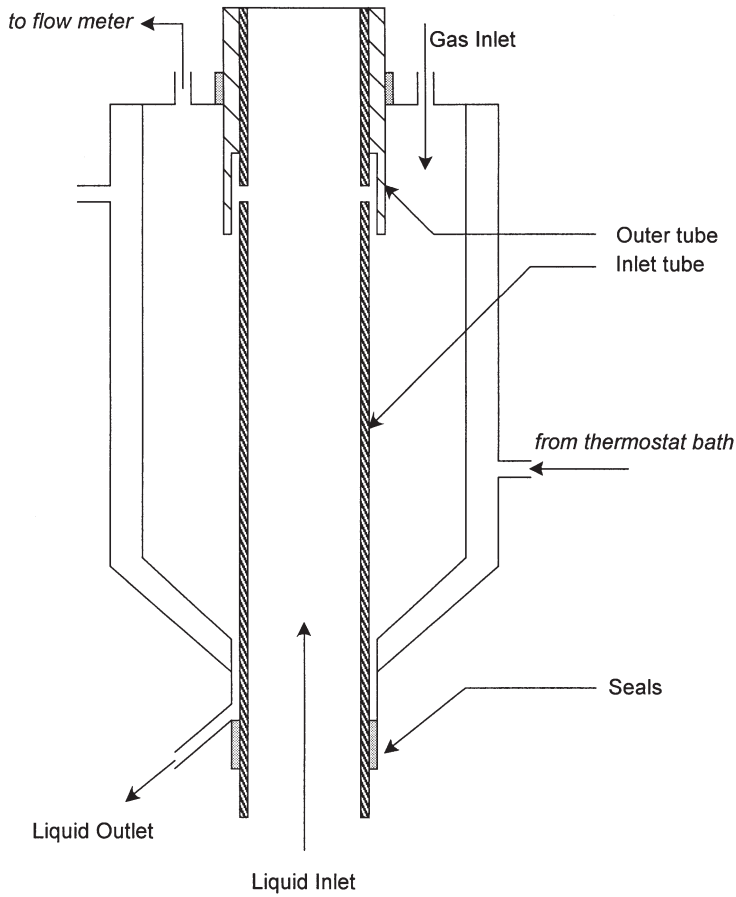

Figure 8. Schematic representation of the wetted wall column. Liquid flows as a falling film along the outer wall of the inner tube.

outer tube surface. After coming in contact with the gas, the liquid was collected at the bottom of the contactor and then transferred to a storage vessel for regeneration.

CO_2 gas from a cylinder was presaturated by passing it through a double-walled vessel maintained at the same temperature as the reactor. The vessel was filled with the liquid under investigation. The presaturated gas was then fed to the reactor. The gas outlet was fitted with a soap film meter to measure the gas flow rate. The meter was also made of double-walled glass and could be maintained at the same temperature as the contactor with the help of water from the thermostat bath. From the exit, the gas is led to a vent.

(Partly) saturated liquid was pumped to a storage vessel where it was stripped of the absorbed gas by means of a vacuum pump. The regenerated liquid was then reused for further experiments.

Experimental Procedure. Once steady state with respect to liquid flow and the desired temperature was achieved, presaturated CO_2 was fed into the contactor. The gas is allowed to flow for some time to exclude all inerts from the reactor, after which the gas inlet and outlet are closed. The soap film meter is then used to measure the volumetric rate of gas absorption into the liquid. Since the contactor is completely isolated from its surroundings, the only way for the gas to escape is via absorption into the liquid phase. Absorption rates for a given gas-liquid system were determined for different lengths of the falling film and liquid flow rates. All experiments were carried out at atmospheric pressure and 293 K.

Results

The wetted wall column described in this study was used to measure the absorption of CO_2 in four different liquid systems, namely, demineralized water, ethanol, n-heptane and MTBE. The physical parameters of these liquids are given in Table II. A typical absorption pattern of CO_2 along the length of the falling film is shown in Figure 9 for the case of ethanol. Here, the square of the absorption rate $W^2_{CO_2}$ is plotted against L. As indicated by Equation (15b), the diffusion coefficient can then be determined from the slope of the line. As seen from the figure, there is no noticeable stagnant zone along the length of the film. In addition, absorption rates at shorter film lengths can be used to determine the molecular diffusion coefficient, while those at longer film lengths give the effective diffusion coefficient, as these points lie within the nonideal zone of the falling film. The intercept of the latter, along the x-axis, indicates the length of the operating zone.

Table II Physical parameters of liquids at 293 K; taken from Daubert and Danner (1985)

Parameter	Units	H_2O	Ethanol	MTBE	n-Heptane
m_{CO_2}	–	0.94	2.64	4.19	1.91
ρ_L	$kg\,m^{-3}$	996.3	790.4	740.7	685.9
η_L	Pa s	$1.02\ 10^{-3}$	$1.19\ 10^{-3}$	$3.56\ 10^{-4}$	$4.06\ 10^{-4}$
σ_L	$N\,m^{-1}$	$7.38\ 10^{-2}$	$2.24\ 10^{-2}$	$1.97\ 10^{-2}$	$2.03\ 10^{-2}$

Values experimentally determined at 293 K.

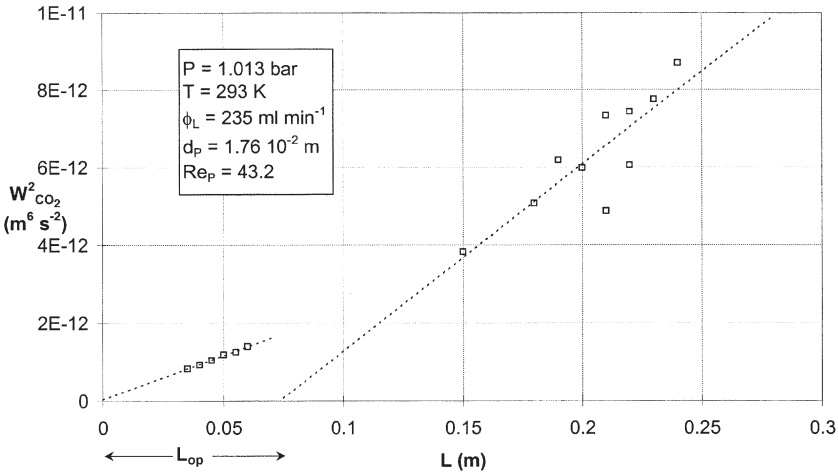

Figure 9. Typical absorption pattern along the length of the falling film (Wetted Wall Column; CO_2-ethanol system). D_{CO_2} as determined from operating zone $= 2.49\,10^{-9}\,m^2\,s^{-1}$. Intercept along x-axis used to determine length of the operating zone.

Absorption of CO_2 within the Operating Zone. Figure 10 gives the results of the molecular diffusion coefficient for three different gas-liquid systems as a function of the Reynolds number. For these diffusion coefficients, absorption only within the operating zone was used to exclude turbulence and rippling effects. As is seen from the figure, the molecular diffusion coefficient remains dependent on experimental conditions (i.e., the Reynolds number) even though the falling film is laminar and without any ripples on the surface. The influence of increasing the Reynolds number also differs from liquid to liquid. While for water and ethanol there is a gradual reduction in diffusivity with an increase in Re_P, the trend was found to be opposite for n-heptane. The average diffusion coefficient for n-heptane over the range of Reynolds numbers studied was found to be $3.68\,10^{-9}\,m^2\,s^{-1}$, which is lower than the value of $6.89\,10^{-9}\,m^2\,s^{-1}$ reported by Takeuchi et al. (1975) using a diaphragm cell. A comparison of diffusivities of CO_2 in ethanol obtained in the present study with values reported previously in literature is given in Table I.

The diffusion coefficients for MTBE are not reported here since the order of magnitude of the experimental diffusivities found were higher than that usually expected for diffusion coefficients of gases in liquids. In addition, the diffusivities were found to be strongly dependent on the value of Re_P, indicating that the liquid film starts rippling immediately on entering the reactor so that the formation of the operating zone does

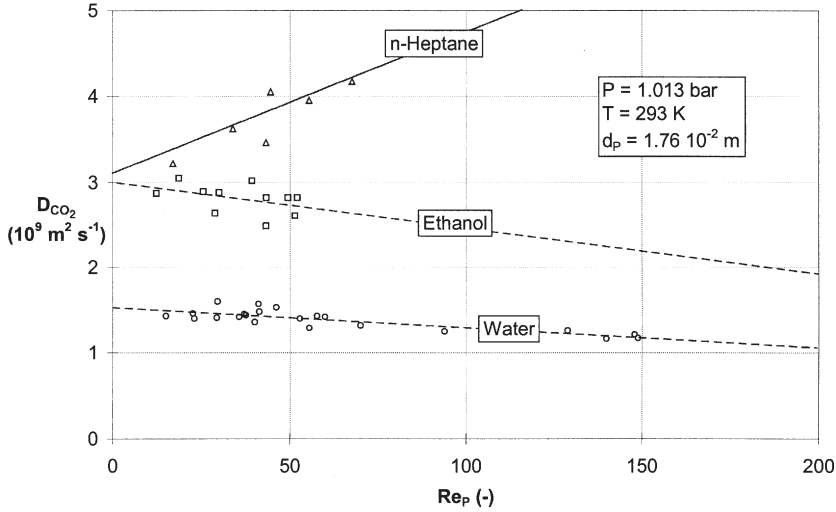

Figure 10. Influence of Reynolds number on diffusivity of CO_2. (Wetted Wall Column). All measurements conducted within the operating zone. Fitted results are: Water: $D_{CO_2} = 1.533\,10^{-9} - 2.433\,10^{-12}(\mathrm{Re}_P)$; Ethanol: $D_{CO_2} = 2.970\,10^{-9} - 3.620\,10^{-13}(\mathrm{Re}_P)$; n-Heptane: $D_{CO_2} = 3.110\,10^{-9} + 1.638\,10^{-11}(\mathrm{Re}_P)$.

not occur. Consequently, the diffusivities observed for MTBE are best interpreted as effective diffusion coefficients.

The presence of the operating zone was, however, visually observed for all three liquids reported in Figure 10. The method of determining the length of the operating zone from absorption data is given above. The length of the operating zone was found to be dependent on the liquid flow rate and was correlated by Equation (13). Figures 11a and 11b depict the variation in the length of the operating zone with the Reynolds number for ethanol and n-heptane, respectively.

As mentioned above, Equations (16a) and (16b) have been derived for flat plate geometry. In order to check the influence of the radius of curvature of the inlet pipe on the velocity profile, absorption of CO_2 in water was carried out in a wetted wall column with a larger inlet pipe (30 mm). Molecular diffusivities obtained with the larger pipe were the same as those reported in Figure 10, indicating that the influence of radius of curvature on the overall absorption was negligible and the use of Equations (16a) and (16b) was valid for the investigations presented in this study. However, the use of a large inlet pipe resulted in a smaller length of the operating zone so that the ripples on the film surface occurred very close to the liquid inlet.

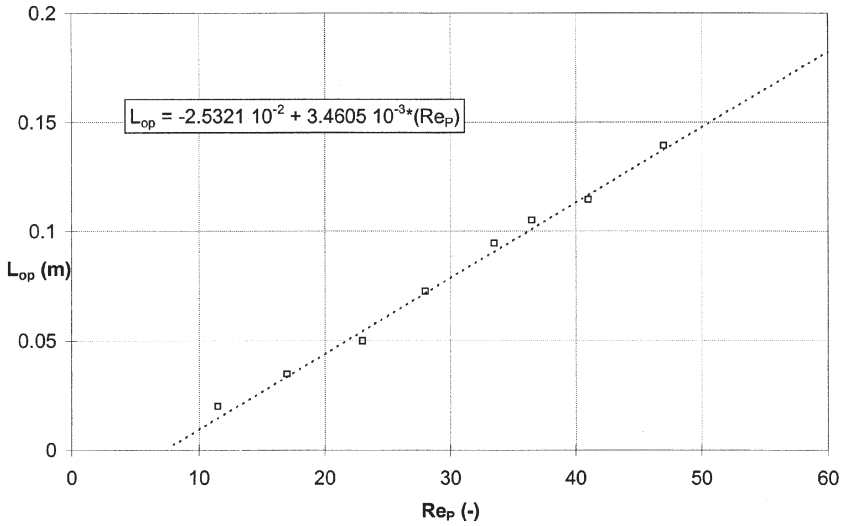

Figure 11a. Length of the operating zone as a function of the Reynolds number (Wetted Wall Column; CO_2-ethanol system).

Absorption of CO_2 within the Nonideal Zone. A kind of effective diffusion coefficient can be determined using the absorption measurements carried out within the nonideal zone. As indicated above, the effective diffusion coefficient of CO_2 can be correlated by Equation (17), with the enhancement in molecular diffusion being linearly dependent on the Reynolds number. The effective diffusion coefficient for the CO_2-ethanol, CO_2-n-heptane and CO_2-MTBE systems is presented in Figures 12a, 12b and 12c, respectively. As can be observed in the figures, there is a steady rise in the effective diffusivity, which can be explained by the increase in absorption rate due to either the increase in interfacial area by the formation of ripples on the interface, or the enhancement in molecular diffusivity by turbulence. As seen from Figures 12a and 12b, the y-intercept value of the effective diffusivity ($Re \rightarrow 0$) correlates (fairly) well with the value of the molecular diffusion coefficient for ethanol and n-heptane (Figure 10). Assuming the same trend to be valid for MTBE, it follows from Figure 12c that the molecular diffusion coefficient of CO_2 in MTBE is of the order of $2.41\ 10^{-9}\ m^2\ s^{-1}$.

DISCUSSION

The influence of liquid Reynolds number on molecular and effective diffusivity has been presented here for gas absorption in model gas-liquid contactors with well-defined hydrodynamics. The influence of Reynolds

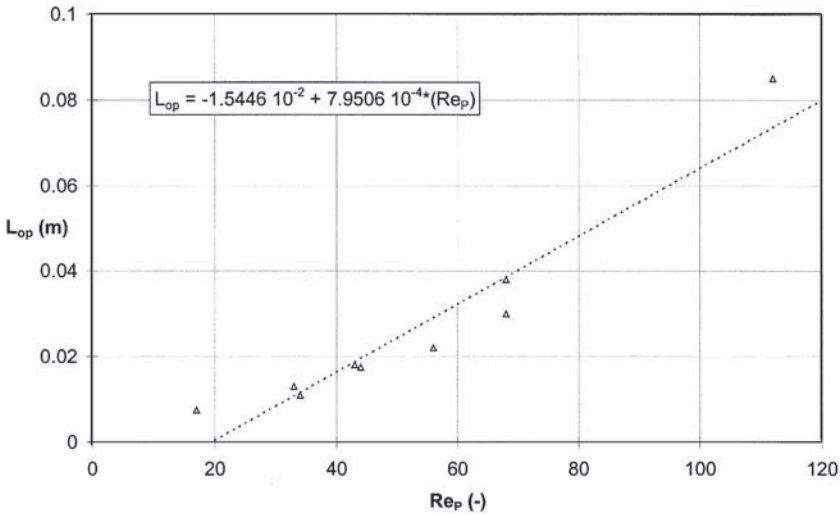

Figure 11b. Length of the operating zone as a function of the Reynolds number (Wetted Wall Column; CO_2-n-heptane system).

number on the effective diffusivity can be explained by the increasing contribution of eddy diffusivity on the overall mass transfer with an increase in Re_P. This explains the rise in effective diffusivity as seen in Figures 12a and 12b. This increase is also a result of an increased surface area due to the formation of ripples on the gas-liquid interface.

However, the change in the molecular diffusion coefficient with Reynolds number cannot be explained by the usual mass transfer theories, namely, the film theory and the surface renewal theories. These theories assume that for a liquid in the laminar regime, the transport of a gas is mainly controlled by molecular diffusivity. The contribution of turbulence (if any) is not accounted for at these low Reynolds numbers. Such a restriction is avoided by the model presented by King (1966), who proposed mass transfer in the vicinity of a gas-liquid interface to occur by a combination of both molecular diffusivity and turbulent transport in the form of small eddies. The effective diffusivity (within the laminar regime) can then be described as

$$D^L_{A,eff} = D_A + py^n \tag{18}$$

where py^n represents the contribution of eddy diffusivity.

This contribution varies with distance y perpendicular to the gas-liquid interface. If one assumes a zone near the interface where all resistance to mass transfer is present, then eddies causing surface renewal

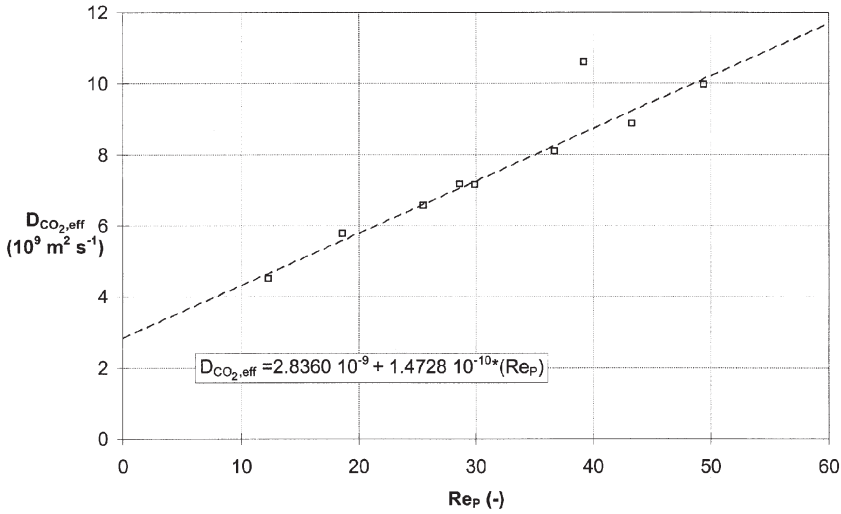

Figure 12a. Variation of the effective diffusion coefficient with Reynolds number. All measurements conducted within the nonideal zone. (wetted wall column; CO_2-ethanol system).

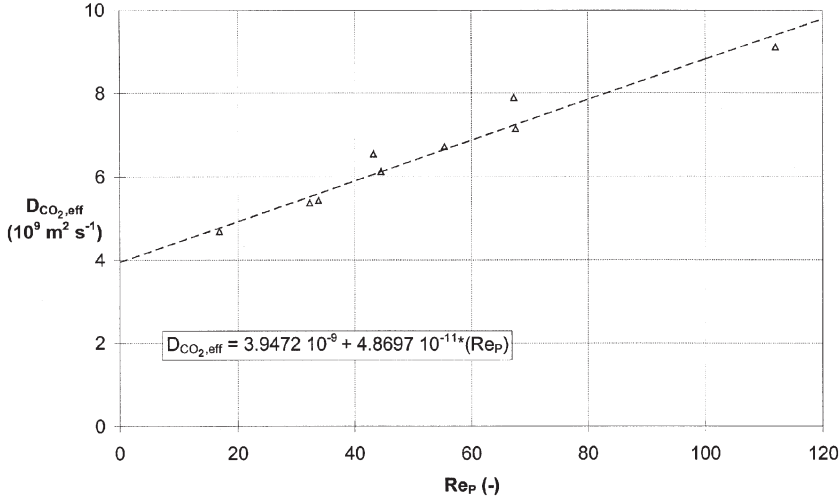

Figure 12b. Variation of the effective diffusion coefficient with Reynolds number. All measurements conducted within the nonideal zone. (wetted wall column; CO_2-n-heptane system).

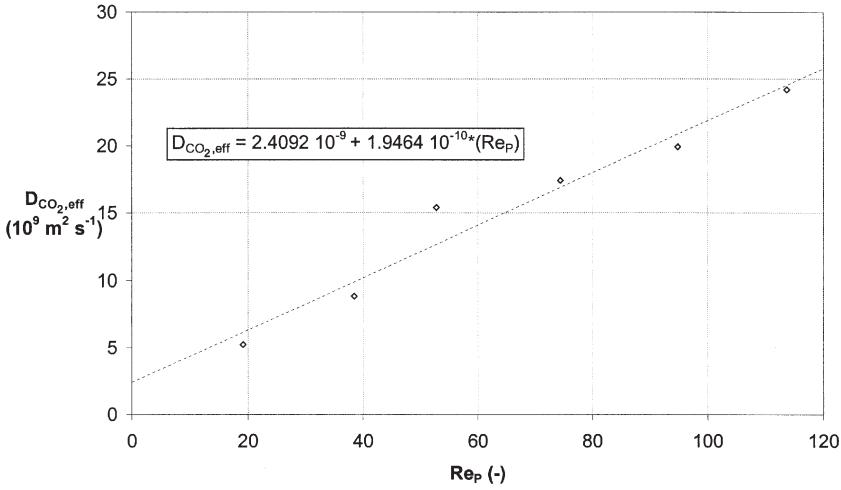

Figure 12c. Variation of the effective diffusion coefficient with Reynolds number. Operating zone is not observed. (wetted wall column; CO_2-MTBE system).

would be large in size as compared to the thickness of the zone, while eddies responsible for eddy diffusivity would be smaller in size than this thickness. The overall effect of all eddies of the same size as that of the resistance zone would be a combination of surface renewal and eddy diffusivity.

It would seem likely that the influence of eddy diffusivity on the overall absorption would reduce closer to the gas-liquid interface. This dampening of the eddies could occur due to the surface tension of the liquid, which might severely reduce the effect of smaller eddies that contribute to eddy diffusivity. In general, the lower surface tension of the organic liquids investigated here could explain the stronger variation in diffusivity with Reynolds number for these liquids (Figures 5 and 10). The higher surface tension of water dampens the eddies near the interface so that the overall transport is mainly governed by molecular diffusion only.

For the case of absorption of CO_2 in n-heptane (Figure 10), the increase in diffusivity with Re_P can be explained on the basis of enhancement to mass transfer caused by eddy diffusivity. Unfortunately, one cannot explain the reduction in diffusion coefficient seen for the case of ethanol in both laminar jet and the wetted wall column with an increase in liquid Reynolds number.

Other typical interfacial phenomena that are known to influence gas absorption are those caused by surface tension gradients (Marangoni effect) and density gradients (Rayleigh effect) that can occur due to the

absorption of a gas. However, the contribution of these effects (though large in some cases) is difficult to quantify.

In conclusion, it is clear that absorption of gases in aqueous and nonaqueous solvents in model laminar jets and falling films cannot be completely explained by conventional mass transfer theories. Some of the observed phenomena could be attributed to the occurrence of eddy diffusivity along with molecular transport and/or the presence of Rayleigh and Marangoni effects. These explanations cannot, however, be validated quantitatively. The experiments presented here do indicate that greater caution should be exercised when using these model contactors for physical absorption and kinetic experiments. Especially for experiments concerned with mass transfer with simultaneous chemical reaction, phenomena such as interfacial turbulence could enhance the overall mass transfer even when the reactor is operated well within the laminar regime. Subsequently, absorption data could be misinterpreted as being enhanced by chemical reaction.

CONCLUSIONS

The application of the laminar jet and wetted wall column for the determination of diffusivity of gases in nonaqueous liquids has been investigated. The absorption of CO_2 in ethanol, n-heptane and MTBE has been used for this purpose. Absorption experiments have been carried out within the laminar and transition regime for both types of reactors. The resulting diffusion coefficient has been found to vary with the Reynolds number within the laminar region. In the case of ethanol, the value of diffusivity reduces with an increase in Reynolds number, while this trend is reversed for n-heptane. Molecular diffusivity in MTBE could not be determined as the rippling of the jet commenced at the top of the column. Absorption under turbulent conditions can be described by an effective diffusivity that has been found to increase with Reynolds number for all liquids investigated.

It is not possible to explain the nonideal behavior of the diffusion coefficient with respect to the Reynolds number with the data available at present. One explanation possible is that the overall mass transfer (in the laminar regime) is governed by a combination of molecular diffusivity and eddy diffusivity as proposed by the model of King (1966). The lower surface tension of the nonaqueous solvents reduces the dampening of eddies and allows them to be present in the vicinity of the gas-liquid interface.

In general, it is clear that data on the absorption of gases into organic and nonaqueous liquids obtained from model contactors should be regarded with caution with respect to the phenomena occurring at the gas-liquid interface.

NOMENCLATURE

a	specific gas-liquid interfacial area, $m^2\,m^{-3}$
C_A	concentration of component A, $mol\,m^{-3}$
d	diameter, m
He	Henry coefficient, $mol\,m^{-3}\,Pa^{-1}$
k_L	liquid side mass transfer coefficient, $m\,s^{-1}$
L	length, m
m_A	gas partition coefficient, defined by (15c)
n	exponent of eddy diffusivity, defined by (18)
N_A	gas absorption flux, $mol\,m^{-2}\,s^{-1}$
p	pressure, Pa
R	jet radius, m
R_A	gas absorption rate, $mol\,s^{-1}$
Re_C	critical Reynolds number, defined by (3a) and (3b)
Re_J	jet Reynolds number, defined by (9)
Re_P	wetted wall Reynolds number, defined by (11b)
T	temperature, K
t	time variable s
U	average liquid velocity, $m\,s^{-1}$
v	liquid velocity, $m\,s^{-1}$
V_L	liquid volume, m^3
W_A	volumetric gas absorption rate, $m^3\,s^{-1}$
x	place variable, m
y	perpendicular distance from interface, m

Greek letters

δ	thickness of falling film, m
ΔD	increase in molecular diffusion, defined by (17), $m^2\,s^{-1}$
ϕ	flow rate, $m^3\,s^{-1}$
Γ	volumetric flow rate per unit wetted perimeter, $m^2\,s^{-1}$
η_L,	liquid viscosity, Pa s
ρ	density, $kg\,m^{-3}$
σ	standard deviation
σ_L	liquid surface tension, $N\,m^{-1}$
τ	gas-liquid contact time, s
ξ	function, defined by (1), $s^{(\Psi-1)}\,m^{(1-2\Psi)}$
Ψ	exponent, defined by (1)

Superscript

L	laminar

Subscripts

0	initial
A	gas component, A
eff	effective
G	gas, gas bulk
i	interface
J	jet
L	liquid
n	nozzle
op	operating zone
P	pipe

REFERENCES

Alvarez-Fuster, C., Midoux, N., Laurent, A. and Charpentier, J. C. (1981). Chemical Kinetics of the Reaction of CO_2 with Amines in Pseudo m-nth Order Conditions in Polar and Viscous Organic Solutions, *Chem. Eng. Sci.*, **36**, 1513–1518.

Danckwerts, P. V. (1951). Significance of Liquid-Film Coefficients in Gas Absorption, *Ind. Eng. Chem.*, **43**, 1460–1467.

Daubert, T. E. and Danner, R. D. eds. (1985). *Data Compilation Tables of Properties of Pure Components*, American Institute of Physical Engineers, New York.

Duda, J. L. and Vrentas, J. S. (1967). Fluid Mechanics of Laminar Liquid Jets, *Chem. Eng. Sci.*, **22**, 855–869.

Fogg, P. G. T. and Gerrard, W. (1991). *Solubility of Gases in Liquids*, Wiley, England.

Higbie, R. (1935). The Rate of Absorption of a Pure Gas into a Still Liquid during Short Periods of Exposure, *Trans. AIChE.*, **35**, 36–60.

King, C. J. (1966). Turbulent Liquid Phase Mass Transfer at a Free Gas-Liquid Interface, *Ind. Eng. Chem. Fund.*, **5**, 1–8.

Nielsen, C. H. E., Kiil, S., Thomsen, H. W. and Dam-Johansen, K. (1998). Mass Transfer in Wetted-Wall Columns: Correlations at High Reynolds Numbers, *Chem. Eng. Sci.*, **53**, 495–503.

Reid, R. C., Prausnitz, J. M. and Poling, B. E. (1988). *The Properties of Gases and Liquids*, 4th ed., McGraw-Hill, Singapore.

Sande, E. van de and Smith, J. M. (1976). Jet Break-Up and Air Entrainment by Low Velocity Turbulent Water Jets, *Chem. Eng. Sci.*, **31**, 219–224.

Schlichting, H. (1968). *Boundary-Layer Theory*, McGraw-Hill, New York.

Scriven, L. E. and Pigford, R. L. (1959). Fluid Dynamics and Diffusion Calculations for Laminar Liquid Jets, *AIChE J.*, **5**, 397–402.

Simons, J. and Ponter, A. B. (1975). Diffusivity of Carbon Dioxide in Ethanol-Water Mixtures, *J. Chem. Eng. Japan*, **8**, 347–350.

Snijders, E. D., te Riele, M. J. M., Versteeg, G. F. and van Swaaij, W. P. M. (1995). Diffusion Coefficients of CO, CO_2, N_2O and N_2 in Ethanol and Toluene, *J. Chem. Eng. Data*, **40**, 37–39.

Spedding, P. L. and Jones, M. T. (1988). Heat and Mass Transfer in Wetted-Wall Columns: I, *Chem. Eng. J.*, **37**, 165–176.

Takahashi, M., Kobayashi, Y. and Takeuchi, H. (1982). Diffusion Coefficients and Solubilities of Carbon Dioxide in Binary Mixed Solvents, *J. Chem. Eng. Data*, **27**, 328–331.

Takeuchi, H., Fujine, M., Sato, T. and Onda, K. (1975). Simultaneous Determination of Diffusion Coefficient and Solubility of Gas in Liquid by a Diaphragm Cell, *J. Chem. Eng. Japan*, **8**, 252–253.

Tang, Y. P. and Himmelblau, D. M. (1965). Effective Binary Diffusion Coefficients in Mixed Solvents, *AIChE J.*, **11**, 54–58.

Toor, H. L. and Marchello, J. M. (1958). Film-Penetration Model for Mass Transfer and Heat Transfer, *AIChE J.*, **4**, 97–101.

Treybal, R.E., *Mass Transfer Operations*, 3rd ed., McGraw-Hill, New York, 1980.

Versteeg, G. F. and van Swaaij, W. P. M. (1988a). Solubility and Diffusivity of Acid Gases (CO_2, N_2O) in Aqueous Alkanolamine Solutions, *J. Chem. Eng. Data*, **33**, 29–34.

Versteeg, G. F. and van Swaaij, W. P. M. (1988b). On the Kinetics between CO_2 and Alkanolamines Both in Aqueous and Non-Aqueous Solutions — I. Primary and Secondary Amines, *Chem. Eng. Sci.*, **43**, 573–585.

Whitman, W. G. (1923). Preliminary Expreimental Confirmation of the Two-Film Theory of Gas Absorption, *Chem. Met. Eng.* **29**, 146–148.

Yoshimura, P. N., Nosoko, T. and Nagata, T. (1996). Enhancement of Mass Transfer into a Falling Laminar Liquid Film by Two-dimensional Surface Waves — Some Experimental Observations and Modelling, *Chem. Eng. Sci.*, **51**, 1231–1240.